Improved synthesis and characterization of cholesteryl oleate-loaded cationic solid lipid nanoparticles with high transfection efficiency for gene therapy applications

Marc Suñé-Pou[1,2,3], Isaac Nofrerias[1], Anna Nardi-Ricart[1], Silvia Prieto-Sánchez[2], Younes El-Yousfi[2], Pilar Pérez-Lozano[1,3], Encarna García-Montoya[1,3], Montserrat Miñarro-Carmona[1,3], Josep Ramón Ticó[1,3], Cristina Hernández-Munain[4], Carlos Suñé[2,*], and Josep Mª Suñé-Negre[1,3]

[1]Service of Development of Medicines (SDM). Faculty of Pharmacy, University of Barcelona. Avda. Joan XXIII, s/n 08028 Barcelona, Spain.

[2]Department of Molecular Biology, Institute of Parasitology and Biomedicine "López-Neyra" (IPBLN-CSIC), PTS, 18016 Granada, Spain.

[3]Pharmacotherapy, Pharmacogeneteics and Pharmaceutical Technology Research Group. IDIBELL-UB, Duran i Reynals Hospital, 3ª level, Gran Via de l'Hospitalet 199, 08908 Hospitalet de Llobregat, Barcelona, Spain.

[4]Department of Cell Biology and Immunology, Institute of Parasitology and Biomedicine "López-Neyra" (IPBLN-CSIC), PTS, 18016 Granada, Spain.

[*]Corresponding author: Telephone: +34 958181645, Fax: +34 958181632 E-mail: csune@ipb.csic.es

ABSTRACT

The development of new nanoparticle formulations that are capable of high transfection efficiency without toxicity is essential to provide new tools for gene therapy. However, the issues of complex, poorly reproducible manufacturing methods, and low efficiencies during *in vivo* testing have prevented translation to the clinic. We have previously reported the use of cholesteryl oleate as a novel excipient for solid lipid nanoparticles (SLNs) for the development of highly efficient and nontoxic nucleic acid delivery carriers. Here, we performed an extensive characterization of this novel formulation to make the scale up under Good Manufacturing Practice (GMP) possible. We also describe the complete physicochemical and biological characterization of cholesteryl oleate-loaded SLNs to ensure the reproducibility of this formula and the preservation of its characteristics before and after the lyophilization process. We defined the best manufacturing method and studied the influence of some parameters on the obtained nanoparticles using the Quality by Design (ICH Q8) guideline to obtain cholesteryl oleate-loaded SLNs that remain stable during storage and guarantee *in vitro* nucleic acid delivery efficacy. Our results indicate that this improved formulation is suitable for gene therapy with the possibility of scale-up the manufacturing of nanoparticles under GMP conditions.

Keywords: cholesteryl oleate, solid lipid nanoparticles, physicochemical characterization, Quality by Design, QbD, stability study, storage conditions, gene therapy, transfection efficiency.

1. Introduction

The administration of DNA and RNA molecules to modulate the expression of proteins is a promising approach for the treatment of several human disorders such as cancer, cystic fibrosis and multiple sclerosis (Naldini, 2015). Nucleic acid-based therapies can replace mutated genes by gene replacement and increase or decrease protein function by gene overexpression or RNA interference (RNAi) gene suppression, respectively. Despite remarkable *in vitro* and *in vivo* results using nucleic acid delivery systems, the translational progress for medical applications has been limited mainly due to poor delivery efficiency and complex manufacturing methods. Addressing the barriers associated with delivery efficiency is a challenge that needs to be overcome for the clinical translation of nucleic acid-based systems. Although many approaches have been taken for the development of safe, reproducible, robust, and efficient new delivery systems, the percentage of success is limited, and additional research to meet the delivery, safety, and industry challenges is required (Wilhelm et al., 2016). The research and use of nanoparticles in the biomedical field as nonviral vectors for the delivery of nucleic acids has become very important in recent decades. Different types of nanoparticles can be engineered with distinctive materials, compositions, and physicochemical properties to enable the cellular uptake of biomolecules for a wide range of biological applications.

Among nanoparticle-based methods, cationic solid lipid nanoparticles (cSLNs) are one of the most promising systems for gene therapy (del Pozo-Rodríguez et al., 2016) (Suñé-Pou et al., 2017)(Nayerossadat et al., 2012). Several advantages have been associated with the use of cSLNs as carriers: i) good biocompatibility and low cytotoxicity (Dolatabadi et al., 2014) (Geszke-Moritz and Moritz, 2016); ii) the possibility of transfecting DNA and RNA *in vitro* and *in vivo* (De Jesus and Zuhorn, 2015); iii) the possibility of using different administration routes, such as intravenous, intramuscular,

oral, topical, nasal, pulmonary or ocular routes (Weber et al., 2014) (Apaolaza et al., 2016) (Kang et al., 2018) (Zhao et al., 2018) (Ferreira et al., 2017) (Ren et al., 2013) (Alvarez-Trabado et al., 2017); iv) the capability to be functionalized to enhance therapeutic effects (Rostami et al., 2014); and v) the possibility of using safe, reproducible, and robust manufacturing methods (Müller et al., 2000).

The cSLNs are spherical vesicles based on oil-in-water microemulsions and, generally consist of a lipid core and a surfactant that stabilizes the particle in an aqueous environment (Hou et al., 2003)(Kumar and Randhawa, 2013). The use of cationic lipids leads to a positive charge on the nanoparticle surface, which mediates the binding of nucleic acids for SLNplex formation. Compatibility among the excipients and the active biomolecules is of high importance and can greatly affect the particle size and zeta potential of nanoparticles and the stability of the formulation (Sznitowska et al., 2017) (Karn-orachai et al., 2016). Appropriate preformulation studies and the characterization of the final formulation are required to ensure good compatibility among the nanoparticle components and the adequate stability of the final product. Analogously, the cSLN manufacturing method is also of critical importance. Several different approaches have been developed to produce cSLNs with potential good therapeutic use; however, most of these nanoparticles are made in small batches using labor-intensive, time-consuming, and high-cost methods. While these engineered materials are adequate for early experimental studies, this limits the translation of promising nanomaterials to clinical applications, where scale-up, reliability, and cost-effective manufacturing to meet the Good Manufacturing Practice (GMP) and the International Council for Harmonization of Technical Requirements for Pharmaceuticals for Human Use (ICH) standards are required. The concept of the ICH Q8 guideline is based on defining a design space, which consists of evaluating the impact of material attributes and process parameters on

manufacturability and the critical quality attributes of final products (European Medicines Agency, 2015)(Huang et al., 2009). According to Quality by Design (QbD), the quality of a product must be "built into" the product and ensured since the design, through an extensive mechanistic understanding of the relations between the product quality and parameters, can have an impact on the quality (Tomba et al., 2013).

We have recently proposed the use of a cholesterol derivative, cholesteryl oleate, in cSLN-nucleic acid formulations to improve the cytotoxicity and transfection efficiency as an avenue for the development of highly efficient and biocompatible carriers for therapeutic purposes (Suñé-pou et al., 2018). The present study conducted an extensive *in vitro* and *in vivo* characterization of this novel formulation to show its feasibility for successful manufacturing scale-up. The process described here establishes a reproducible and robust process for the synthesis of novel and stable cholesteryl oleate-loaded cSLNs that are suitable for manufacturing and comply with GMP guidelines for potential use in clinical applications.

2. Materials and methods

2.1. cSLN production

The following materials were used to synthesize the nanoparticles: poloxamer 188 (Sigma-Aldrich Co., St Louis, MO, USA), octadecylamine (Acros Organics, Geel, Belgium), stearic acid (EMD Millipore, Billerica, MA, USA), cholesteryl oleate (Alfa Aesar, Karlsruhe, Germany) and ultrapure water (EMD Millipore).

The proportions of all components of the formulation were as follows: 200 mg of stearic acid, 300 mg of cholesteryl oleate, 600 mg of octadecylamine, and 100 mg of poloxamer 188. The cSLNs were produced using the hot microemulsification method, as previously described (Fàbregas et al., 2014). First, all the components were heated and melted at 80

°C. In separate receptacles, we added the matrix lipids (stearic acid and cholesteryl oleate), the cationic lipid, the poloxamer 188, and 20 mL of Milli-Q water. When all components were melted and had reached the same temperature, the matrix lipids were poured into the second receptacle with stirring at 20.000 rpm (IKA® T-25 Digital Ultra-Turrax®, S25N-8G rotor) for 10 min. The emulsion that was obtained was dispersed into 125 mL of cooled water at 4 °C under the same stirring conditions. In this phase, nanoparticles were formed. This final nanoemulsion was centrifuged at 19,000 x g at 4 °C for 30 min and then filtered through 43-48 µm filters (FILTER-LAB®, Filtros ANOIA, S.A. Barcelona). The final nanoparticle suspension was mixed with a solution of 5% trehalose to lyophilize it, to improve its stability and to preserve its properties during the lyophilization process using an L-3 Telstar (Spain) laboratory freeze dryer system.

2.2 Improvement of the manufacturing method

To improve the manufacturing method, several changes were introduced during different steps of the process by employing QbD methodologies. Risk assessment was used throughout development using the SMEA protocols to identify potentially high-risk formulation and process variables. A follow-up study of particle size and zeta potential was performed to evaluate the impact of these modifications on the final product. The main positive changes involved the temperature of the water to pour the first emulsion and temperature of the centrifugation step.

2.3. Stability study

Particle size and zeta potential values were determined when the suspension of nanoparticles was stored at 4, 25 and 37 °C. Similarly, particle size and zeta potential values were determined after the lyophilization process when the nanoparticles were stored at RT and 4 °C.

2.4. Physicochemical characterization of the cSLNs

2.4.1. Determination of the particle size

Particle size was determined by laser diffraction according to the Mie theory on a Mastersizer 2000 (Malvern Instruments, UK). All samples were measured in triplicate using a sufficient amount of sample to obtain an appropriate obscuration percentage. A Fourier transform was applied to the measured diffracted angles to obtain the particle size data using specialized software, and the mean value was calculated in nanometers (nm).

2.4.2. Zeta potential

A Zetasizer Nano Z (Malvern Instruments, UK) was used to determine the surface charge of the cSLNs by laser doppler microelectrophoresis. The samples were stabilized at 25 °C prior to a measurement. The electrophoretic mobility between electrodes that were connected to the cell containing the sample was converted to zeta potential values using specific software. The results are expressed in mV.

2.4.3. Transmission electron microscopy (TEM)

The surface and content homogeneity of the cSLNs were analyzed by TEM using a Spirit 120 kV microscope.

2.4.4. X-ray photoelectron spectroscopy

The surface nitrogen percentage in the cSLNs was quantified. X-ray photoelectron spectroscopy (XPS) experiments were performed using a PHI 5500 Multitechnique System (Physical Electronics) with a monochromatic X-ray source (aluminum K-alpha line of 1486.8 eV and 350 W) that was placed perpendicular to the analyzer axis and calibrated using the 3d5/2 line of Ag with a full width at a half maximum (FWHM) of 0.8 eV.

The analyzed area was a circle with a 0.8 mm diameter, and the selected resolution for the general spectra was a pass energy of 187.5 eV and 0.8 eV/ste. For the spectra of the different elements in the depth profile spectra, the resolution was a pass energy of 23.5 eV and 0.1 eV/step. A low energy electron gun (less than 10^3V) was used to discharge the surface when necessary. All measurements were made in an ultrahigh vacuum (UHV) chamber between 5 x 10^{-9} and 2 x 10^{-8} Torr.

2.4.5. Differential scanning calorimetry (DSC)

The possible interactions of the components in the formulation were assessed using DSC. DSC was performed in a DSC-822e (Mettler Toledo) at a heating rate of 10 °C/min over a range from 30 °C to 200 °C using the heat flow method. This DSC mode measures the difference in the temperature between pans and converts it into a heat flow signal after a calibration procedure. The samples were weighed into a 40 µl aluminum pan, and an empty pan was used as a reference. Dry nitrogen (50 ml/min) was used to perform the assay in a nonoxidative atmosphere.

2.4.6. Eutectic point

The eutectic point of the dispersion of the cSLNs and the cSLNs:Agarose was determined by DSC. DSC was performed by freezing the sample from 25 °C to -80 °C at 10 °C/min. The sample was kept at this temperature for 1 min and then heated to 25 °C at 10 °C/min.

2.5. Biological characterization of cSLNs

2.5.1. SLNplex formation (agarose gel)

The analysis of SLNplex formation and loading efficiency of the cSLNs with plasmid DNA (pDNA) was performed by electrophoretic mobility of the samples on agarose gels. SLNplexes were prepared by mixing the cSLNs with the appropriate amount of pDNA. The mixture was kept at RT for 40-45 min to allow the complexes to form. An aliquot of

the mixture was loaded in the agarose gel. DNA mixed with Milli-Q water as a negative control. For electrophoretic separations in agarose gel, agarose D-1 at 0.8% in 1X Tris-acetate-EDTA (TAE) (40 mM Tris-acetate, 1 mM EDTA) with RedSafe® as a nucleic acid staining solution was used. The 6x gel loading dye thas was used (NEB B7025S) comprised 2.5% Ficoll-400, 10 mM EDTA, 3.3 mM Tris-HCl (pH 8.0 @ 25 °C), 0.02% Dye 1 (pink/red) and 0.0008% Dye 2 (blue). Once resolved in agarose gels, sample visualization took place in a GelDoc® EZ Imager (BioRad®, USA) system using BioRad® ImageLab 5.2.1 software.

2.5.2. Confocal microscopy and cell distribution of nanoparticles and SLNplexes

To study the transfection efficiency, confocal microscopy studies were performed using HeLa cells. The cells were grown in 35-mm plates (Falcon) to a confluence of 60-70%. cSLNs and Cy3-labeled siRNA were mixed in a 1.5 ml tube as previously described for pDNA (see section 2.5.1) and added to every well. As a transfection control, Cy3-labeled siRNA (Sigma) was transfected into cells using Lipofectamine 2000. Cy3-labeled siRNA in water was used as a negative control.

After one hour, the cells were harvested and prepared for confocal microscopy using a Leica SP5 spectral confocal laser scanning microscope. Images were analyzed and digitally processed for presentation using LAS AF v2.3.6 software and Adobe Photoshop CS3 Extended v10.0 software, respectively.

3. Results

3.1. Improvement of cSLN production

We identified the temperature of the water that was used to pour the first emulsion as a critical quality attribute (CQA) for process validation using a QbD approach. We tested three different conditions: water at 4 °C (Suñé-pou et al., 2018), 25 °C and 37 °C. We

observed small difference in particle size at 4 °C, 25 °C or 37 °C. The smallest particle size was obtained at 37 °C with a value of approximately 170 nm (Figure 1). The specifications based on the analysis of the particle size distribution during the manufacturing process for this formula are set at 200 ± 50 nm, therefore, all the conditions tested resulted in an attainable particle size. Based on these data, the temperature of 25 °C is suitable for the stirring in the tank and avoids to design controllers for temperature control in the stirred tank. This improved the manufacturing method and further established a working Design Space (DS) for this processing step according to the QbD criteria.

We next assessed the temperature of the centrifugation process. Two conditions were tested: i) centrifugation at 4 °C and ii) centrifugation at RT. No differences were observed in terms of particle size (Table 1). This result avoids the necessity of cooling down the centrifuge and controlling the temperature, thus facilitating the manufacturing method.

3.2. Studies of thermal stability

We first tested the stability of freshly made cSLNs. We observed that storage conditions are important for nanoparticle preservation (Figure 2A). During the first 3 days, the particle size did not significantly change at 4 °C, 25 °C or 37 °C. On day 5, we observed the presence of aggregates at 25 °C, which was also observed on day 7 at 37 °C. The aggregation increased over time, reaching a particle size of approximately 10 µm on day 15 at 25 °C and 37 °C. At 4 °C, the particle size of cSLNs did not change during this time period. We conclude that 4 °C is the most appropriate temperature for the storage of freshly made cSLNs.

We next extended the incubation time at 4 °C and observed the formation of aggregates on day 18, which was maximized on day 24 (Figure 2B). This result prompted us to perform a stability study using lyophilization to preserve cSLN integrity. After

lyophilization, the nanoparticles were monitored at 4 °C and 25 °C, which are favorable temperature conditions for drug storage and maintenance. The particle sizes of these cSLNs were analyzed after resuspending with Milli-Q water after each time point. We did not observe a change in particle size as far as one year after the study, which demonstrates that the addition of the trehalose cryoprotectant to the cSLNs preserved efficacy, even when reconstituted in pure Milli-Q water (Figure 2C).

3.3. Physicochemical characterization

The particle size was determined several times, and a size of 207 ± 40 nm was achieved (Table 2). Furthermore, the presence of aggregates was not observed, demonstrating that centrifugation and filtration removed the possible aggregates present in the suspension after fabrication.

For the zeta potential values, the cSLNs exhibited values between 30-40 mV, which are optimum to achieving a good positive surface that is effective for nucleic acid binding. It has been reported that values below 25 mV may present problems for the formation of SLNplexes and for the stability of nanoparticles (Honary and Zahir, 2013).

The TEM images confirm the results obtained with the Mastersizer (Figure 3). The nanoparticles showed a spherical morphology and homogenous surfaces with particle sizes consistent with those determined previously. We did not observe the presence of aggregates in these images, supporting the stability of the resuspended lyophilized particles.

Regarding the surface nitrogen percentage, the XPS results showed the presence of this atom in the nanoparticle surface (Figure 4 and Table 3). These data are relevant because, in the water suspension, this nitrogen will be protonated, thereby allowing the positive charge on the particle surface, which is responsible for the nucleic acid binding capacity.

The compatibility among the components in the formulation was assessed using DSC (Figure 5). The results indicate that there are no interactions among cholesteryl oleate, stearic acid, octadecylamine, and poloxamer 188. Binary mixtures between the components exhibited no exothermic peak, which indicates that there are no physical or chemical interactions and thus validates this formulation for further studies.

The study of the eutectic point was carried out in a suspension of cSLNs and a mixture of cSLNs and 5% trehalose at a ratio of 1:1 (Figure 6). The results showed that the eutectic point of the cSLNs was lower than the eutectic point of the mixture (-16.69 °C versus -29.98 °C). We tested several different cryoprotectants and trehalose was the only one capable of achieving cryopreservation while maintaining a good particle size after resuspension (data not shown). Nevertheless, the lyophilization process begins at temperatures of -40 °C; therefore, there is a margin of 10 °C to avoid boiling events.

3.4. Biological characterization

Gel electrophoresis retardation assays are widely used to assess the nucleic acid binding efficiency of cSLNs. The presence of unbound free DNA in the gels reflects the binding capacity of the nanoparticles (Figure 7). When the DNA amount was 0.5-1.0 µg, no free DNA was observed in the gel, which indicated that the DNA was completely bound to the cSLNs. When 2 µg of DNA was used, minimal free DNA was observed in the gel, and considerable free DNA was detected in the gel upon loading 5 µg of DNA. Our results confirmed the suitability of these cSLNs for DNA binding.

Confocal microscopy was used to assess the transfection capacity and the cellular localization of cSLNs:RNA SLNplexes in HeLa cells using Cy3-labeled RNA. We observed minimal fluorescence when Cy3-labeled RNA alone was added to the cells (Figure 8A-B). Large and numerous foci were observed in the cytoplasm and nuclei of

cells transfected with the cSLN-Cy3-labeled RNA complexes (Figure 8C-D). These data demonstrate the capacity of this improved formulation to carry and deliver nucleic acids into the cytoplasm and nucleus of cells with high efficiency.

4. Discussion

The nanoformulation of medicinal drugs is of fundamental importance to address pharmaceutical and biopharmaceutical needs for the delivery of clinically relevant molecules. A complete understanding of nanoformulation requires attention to fundamental research to develop efficient carriers for drug delivery applications. For nanoparticles, a good knowledge of materials and fabrication approaches is essential for achieving optimal physicochemical and biological properties to overcome barriers in nanomedicine delivery. Precise, high-resolution nanoparticle characterization is also essential for nanoparticle submission, review, and acceptance of national and international regulatory agencies prior to commercialization.

One of the purposes of this study was to optimize formulations of cholesteryl oleate-loaded cSLNs and their fabrication methods to maximize therapeutic efficacy. Regarding the manufacturing process, we optimized nanoparticle synthesis by working on two critical steps of the protocol: the temperature of water when the first emulsion is poured and the temperature of centrifugation. Both improvements ease the manufacturing process and avoid temperature control during this process. These improvements are also a first step for a further QbD study to establishing a working DS in every step of the manufacturing process. Stability is a critical attribute that plays an important role in the drug development process. Nanoparticle stability must be determined in the formulation itself and for all the parameters involved with storage and shipment, such as heat and time, to produce a product that is safe and effective. A long-term stability study needs to be performed to evaluate the presence of degradation products that may potentially affect

storage and shipment conditions. Suboptimal storage conditions can affect nanoparticle properties and modulate toxicity and bioavailability (Izak-Nau et al., 2015). We performed this study with our formulation and obtained the following conclusions. Nanoparticle suspensions should be stored at 4 °C for the best performance for a maximum of 15 days. However, a lyophilization process must be carried out before these 15 days. Indeed, the lyophilization conditions described here improved long-term stability at 25 °C, where nanoparticles were stable for at least 1 year. Nanoparticle preservation at room temperature overcomes obstacles to cold storage in many rural parts of developing countries, where a great number of the largest research-based pharmaceutical companies have increased efforts to provide access to essential medicines (Hogerzeil et al., 2014 Lancet Glob Health 2014).

As stated previously, the physicochemical properties of candidate nanoparticles must be characterized to achieve preferred conditions for maintaining low toxicity and good bioactivity. Particle size and zeta potential, which are indicative of the particle surface charge, provide useful information about the cellular uptake and toxicity of nanoparticles and are therefore widely used parameters for the validation of the nanoformulations. The working protocol that is described in this manuscript achieved good particle size and positive surface charge and were therefore suitable for further investigation. Spherical morphologies and homogenous surfaces of cSLNs were visible in TEM images that further confirmed our results of particle size using a Mastersizer. The positive charge of the surface that was observed in the zeta potential measurements is due to the surface nitrogen that is found in the formulation. This positive charge will allow SLNplexes to form. We also observed that all the excipients used in the formulation of the cSLNs showed no interactions among the components and, consequently, revealed a good compatibility (Figure 5). Finally, we optimized a lyophilization protocol for cSLNs

loaded with cholesteryl-oleate and compared the long-term stability of lyophilized nanoparticles under different storage conditions. For lyophilization to occur, the temperature of the frozen matrix must be maintained below the eutectic point of the formulation. The choice of the cryoprotectant is critical to preserving the properties of the nanoparticles after resuspension (Fonte et al., 2016). The addition of the trehalose cryoprotectant at 5% w/v in the formula decreased the eutectic point by 10 degrees (from -18 °C to -28 °C), which required the formula to reach temperatures of approximately -40 °C to completely freeze the nanoparticle suspension. In these conditions, cSLNs maintained their physicochemical properties and transfection capacity over time.

Functionalized nanoparticles have been used in biotechnology for nuclear transfection and targeting in nonviral gene delivery applications because they easily enter cells (Ku et al., 2014)(Rostami et al., 2014). However, these nanoparticles are expensive and have complicated procedures. The binding capacity and transfection efficiency results obtained with our optimized cSLN formulation validate the use of these nanoparticles as safe and effective carriers for nonviral nucleic acid delivery. Confocal microscopy images supported this statement, as they showed many intense siRNA-labeled fluorescent dots throughout the cytoplasm and cell nuclei, achieving a transfection efficiency of approximately 50%. These results encourage the use of these nanoparticles for further investigation.

5. Conclusions

The control of process parameters in nanoformulation is essential to achieve efficient, safe, stable, and reproducible formulations. Key synthesis parameters include temperature, mixing, concentrations, and reaction times. We hereby applied several approaches to address these issues and reported a complete characterization of an optimized formulation to produce nanoparticles with GMPs that remain stable during

storage and guarantee *in vitro* nucleic acid delivery efficacy. The improvement of this manufacturing method produced nanoparticles with substantially increased stability compared to nanoparticles obtained by a standard formulation strategy, encouraging their use for gene targeting applications.

Acknowledgments

We are grateful to many colleagues for their helpful suggestions, critical discussions, and comments. This work was supported by grants from the Spanish Ministry of Economy and Competitiveness (grant number BFU2017-89179-R) and the Andalusian Government (Excellence Project BIO-2515/2012) to C.S. and from the Spanish Ministry of Economy and Competitiveness (grant number BFU2016-79699-P) to C.H.M. Support from the European Region Development Fund (ERDF [FEDER]) is also acknowledged. M.S.-P. was supported by a fellowship from the Spanish Ministry of Education (FPU Program).

Disclosure

The authors declare that they have no conflict of interest.

References

Alvarez-Trabado, J., Diebold, Y., Sanchez, A., 2017. Designing lipid nanoparticles for topical ocular drug delivery. Int. J. Pharm. 532, 204–217. https://doi.org/10.1016/j.ijpharm.2017.09.017

Apaolaza, P.S., del Pozo-Rodríguez, A., Solinís, M.A., Rodríguez, J.M., Friedrich, U., Torrecilla, J., Weber, B.H.F., Rodríguez-Gascón, A., 2016. Structural recovery of the retina in a retinoschisin-deficient mouse after gene replacement therapy by solid lipid nanoparticles. Biomaterials 90, 40–49.

https://doi.org/10.1016/j.biomaterials.2016.03.004

De Jesus, M.B., Zuhorn, I.S., 2015. Solid lipid nanoparticles as nucleic acid delivery system: Properties and molecular mechanisms. J. Control. Release 201, 1–13. https://doi.org/10.1016/j.jconrel.2015.01.010

del Pozo-Rodríguez, A., Solinís, M.Á., Rodríguez-Gascón, A., 2016. Applications of lipid nanoparticles in gene therapy. Eur. J. Pharm. Biopharm. 109, 184–193. https://doi.org/10.1016/j.ejpb.2016.10.016

Dolatabadi, J.E.N., Hamishehkar, H., Eskandani, M., Valizadeh, H., 2014. Formulation, characterization and cytotoxicity studies of alendronate sodium-loaded solid lipid nanoparticles. Colloids Surfaces B Biointerfaces 117, 21–28. https://doi.org/10.1016/j.colsurfb.2014.01.055

European Medicines Agency, 2015. ICH guideline Q8 (R2) on pharmaceutical development. Ema/Chmp/Ich/167068/2004 8, 16706. https://doi.org/EMEA/CHMP/167068/2004 - ICH

Fàbregas, A., Sánchez-Hernández, N., Ticó, J.R., García-Montoya, E., Pérez-Lozano, P., Suñé-Negre, J.M., Hernández-Munain, C., Suñé, C., Miñarro, M., 2014. A new optimized formulation of cationic solid lipid nanoparticles intended for gene delivery: Development, characterization and DNA binding efficiency of TCERG1 expression plasmid. Int. J. Pharm. 473, 270–279. https://doi.org/10.1016/j.ijpharm.2014.06.022

Ferreira, M., Barreiros, L., Segundo, M.A., Torres, T., Selores, M., Costa Lima, S.A., Reis, S., 2017. Topical co-delivery of methotrexate and etanercept using lipid nanoparticles: A targeted approach for psoriasis management. Colloids Surfaces B Biointerfaces 159, 23–29. https://doi.org/10.1016/j.colsurfb.2017.07.080

Fonte, P., Reis, S., Sarmento, B., 2016. Facts and evidences on the lyophilization of polymeric nanoparticles for drug delivery. J. Control. Release 225, 75–86. https://doi.org/10.1016/j.jconrel.2016.01.034

Geszke-Moritz, M., Moritz, M., 2016. Solid lipid nanoparticles as attractive drug vehicles: Composition, properties and therapeutic strategies. Mater. Sci. Eng. C. https://doi.org/10.1016/j.msec.2016.05.119

Honary, S., Zahir, F., 2013. Effect of Zeta Potential on the Properties of Nano - Drug Delivery Systems - A Review (Part 2). Trop. J. Pharm. al Res. 12, 265–273. https://doi.org/10.4314/tjpr.v12i2.19

Hou, D.Z., Xie, C.S., Huang, K.J., Zhu, C.H., 2003. The production and characteristics of solid lipid nanoparticles (SLNs). Biomaterials 24, 1781–1785. https://doi.org/10.1016/S0142-9612(02)00578-1

Huang, J., Kaul, G., Cai, C., Chatlapalli, R., Hernandez-Abad, P., Ghosh, K., Nagi, A., 2009. Quality by design case study: An integrated multivariate approach to drug product and process development. Int. J. Pharm. 382, 23–32. https://doi.org/10.1016/j.ijpharm.2009.07.031

Izak-Nau, E., Huk, A., Reidy, B., Uggerud, H., Vadset, M., Eiden, S., Voetz, M., Himly, M., Duschl, A., Dusinska, M., Lynch, I., 2015. Impact of storage conditions and storage time on silver nanoparticles' physicochemical properties and implications for their biological effects. RSC Adv. 5, 84172–84185. https://doi.org/10.1039/c5ra10187e

Kang, X., Chen, H., Li, S., Jie, L., Hu, J., Wang, X., Qi, J., Ying, X., Du, Y., 2018. Magnesium lithospermate B loaded PEGylated solid lipid nanoparticles for improved oral bioavailability. Colloids Surfaces B Biointerfaces 161, 597–605.

https://doi.org/10.1016/j.colsurfb.2017.11.008

Karn-orachai, K., Smith, S.M., Saesoo, S., Treethong, A., Puttipipatkhachorn, S., Pratontep, S., Ruktanonchai, U.R., 2016. Surfactant effect on the physicochemical characteristics of γ-oryanol-containing solid lipid nanoparticles. Colloids Surfaces A Physicochem. Eng. Asp. 488, 118–128. https://doi.org/10.1016/j.colsurfa.2015.10.011

Ku, S.H., Kim, K., Choi, K., Kim, S.H., Kwon, I.C., 2014. Tumor-targeting multifunctional nanoparticles for sirna delivery: Recent advances in cancer therapy. Adv. Healthc. Mater. 3, 1182–1193. https://doi.org/10.1002/adhm.201300607

Kumar, S., Randhawa, J.K., 2013. High melting lipid based approach for drug delivery: Solid lipid nanoparticles. Mater. Sci. Eng. C 33, 1842–1852. https://doi.org/10.1016/j.msec.2013.01.037

Müller, R.H., Mäder, K., Gohla, S., 2000. Solid lipid nanoparticles (SLN) for controlled drug delivery - A review of the state of the art. Eur. J. Pharm. Biopharm. 50, 161–177. https://doi.org/10.1016/S0939-6411(00)00087-4

Naldini, L., 2015. Gene therapy returns to centre stage. Nature 526, 351–360. https://doi.org/10.1038/nature15818

Nayerossadat, N., Ali, P., Maedeh, T., 2012. Viral and nonviral delivery systems for gene delivery. Adv. Biomed. Res. 1, 27. https://doi.org/10.4103/2277-9175.98152

Ren, J., Zou, M., Gao, P., Wang, Y., Cheng, G., 2013. Tissue distribution of borneol-modified ganciclovir-loaded solid lipid nanoparticles in mice after intravenous administration. Eur. J. Pharm. Biopharm. 83, 141–148. https://doi.org/10.1016/j.ejpb.2012.10.018

Rostami, E., Kashanian, S., Azandaryani, A.H., Faramarzi, H., Dolatabadi, J.E.N., Omidfar, K., 2014. Drug targeting using solid lipid nanoparticles. Chem. Phys. Lipids 181, 56–61. https://doi.org/10.1016/j.chemphyslip.2014.03.006

Suñé-Pou, M., Prieto-Sánchez, S., Boyero-Corral, S., Moreno-Castro, C., Yousfi, Y. El, Suñé-Negre, J.M., Hernández-Munain, C., Suñé, C., 2017. Targeting splicing in the treatment of human disease. Genes (Basel). 8. https://doi.org/10.3390/genes8030087

Suñé-pou, M., Yousfi, E., Boyero-, S., Nardi-ricart, A., Nofrerias-roig, I., Pérez-lozano, P., García-montoya, E., Ticó, R., M[a], J., 2018. Cholesteryl oleate-loaded cationic solid lipid nanoparticles as carriers for efficient gene- silencing therapy. Int. J. Nanomedicine 13, 3223–3233.

Sznitowska, M., Wolska, E., Baranska, H., Cal, K., Pietkiewicz, J., 2017. The effect of a lipid composition and a surfactant on the characteristics of the solid lipid microspheres and nanospheres (SLM and SLN). Eur. J. Pharm. Biopharm. 110, 24–30. https://doi.org/10.1016/j.ejpb.2016.10.023

Tomba, E., Facco, P., Bezzo, F., Barolo, M., 2013. Latent variable modeling to assist the implementation of Quality-by-Design paradigms in pharmaceutical development and manufacturing: A review. Int. J. Pharm. 457, 283–297. https://doi.org/10.1016/j.ijpharm.2013.08.074

Weber, S., Zimmer, A., Pardeike, J., 2014. Solid Lipid Nanoparticles (SLN) and Nanostructured Lipid Carriers (NLC) for pulmonary application: A review of the state of the art. Eur. J. Pharm. Biopharm. 86, 7–22. https://doi.org/10.1016/j.ejpb.2013.08.013

Wilhelm, S., Tavares, A.J., Dai, Q., Ohta, S., Audet, J., Dvorak, H.F., Chan, W.C.W.,

2016. Analysis of Nanoparticle Delivery to Tumours. Nat. Rev. 1, 1–12. https://doi.org/10.1038/natrevmats.2016.14

Zhao, B., Gu, S., Du, Y., Shen, M., Liu, X., Shen, Y., 2018. Solid lipid nanoparticles as carriers for oral delivery of hydroxysafflor yellow A. Int. J. Pharm. 535, 164–171. https://doi.org/10.1016/j.ijpharm.2017.10.040

Figure Legends

Figure 1. Effect of the temperature of the solvent and stirring speed on the particle size.

Figure 2. Thermal stability studies of nanoparticles. (A) Freshly made cSLNs were incubated at 4 °C, 25 °C or 37 °C, and particle size was measured at different time points (1-15 days). (B) The same experiment described in A was carried out at 4 °C for 24 days. (C) Lyophilized cSLNs were incubated at 4 °C and 25 °C for 1 year, and particle size was analyzed at different time points after resuspending the cSLNs in Milli-Q water.

Figure 3. TEM image after the reconstitution of lyophilized cSLNs.

Figure 4. XPS depth profile spectra of lyophilized cSLNs.

Figure 5. DSC depth profiles of binary mixes of stearic acid + cholesteryl oleate (A), stearic acid + octadecylamine (B), stearic acid + poloxamer (C), cholesteryl oleate + octadecylamine (D), cholesteryl oleate + poloxamer 188 (E) and octadecylamine + poloxamer 188 (F).

Figure 6. Eutectic point graphs of cSLN suspension (A) and cSLN + 5% Trehalose (B).

Figure 7. cSLNs (lane 1), 500 to 5000 ng of pDNA with (lanes 2-5) or without (lanes 6-9) cSLNs were loaded on a 0.8% agarose gel. The presence of free DNA in the gel reveals

the binding capacity of the nanoparticles. M: Molecular-weight size markers (in kilobase pairs) were the DNA ladder digest (New England Biolabs).

Figure 8. Confocal microscopy images of HeLa cells transfected with Cy3-labeled siRNA (A and B) and SLNplexes of Cy3-labeled siRNA:SLNs (panels C and D). Green, Alexa Fluor® 488 Staining; red, Cy3-labeled siRNA; blue, DAPI staining.

Table 1. Improvement of the manufacturing method. Particle size (nm).

	Centrifugation	
	4 °C	25 °C
1	187	206
2	224	227
3	210	217
Mean	207	216,67
Standard Deviation	18,68	10,50

Table 2. Particle size and zeta potential of the SLNs.

	Particle size (nm)	*Zeta potential (mV)*
	172	39,8
	224	34,0
	255	30,0
	173	33,1
	210	36,9

Mean	207	34,76
Standard Deviation	35,06	3,74

Table 3. Atomic composition (%) of the cSLNs surface

C1s	N1s	O1s	Others
90.3	2.80	6.35	0.55

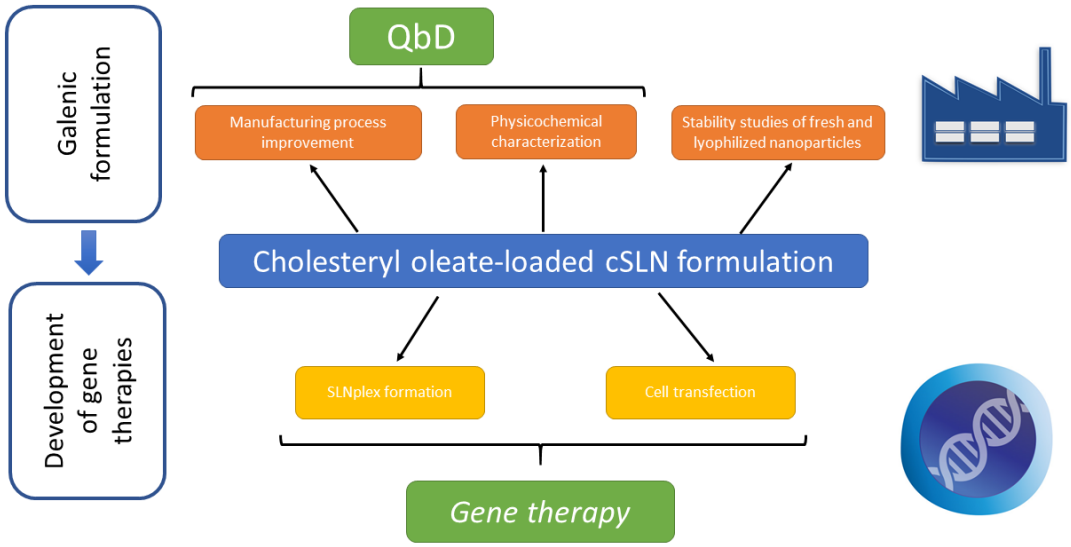

Graphical abstract

Figure 1

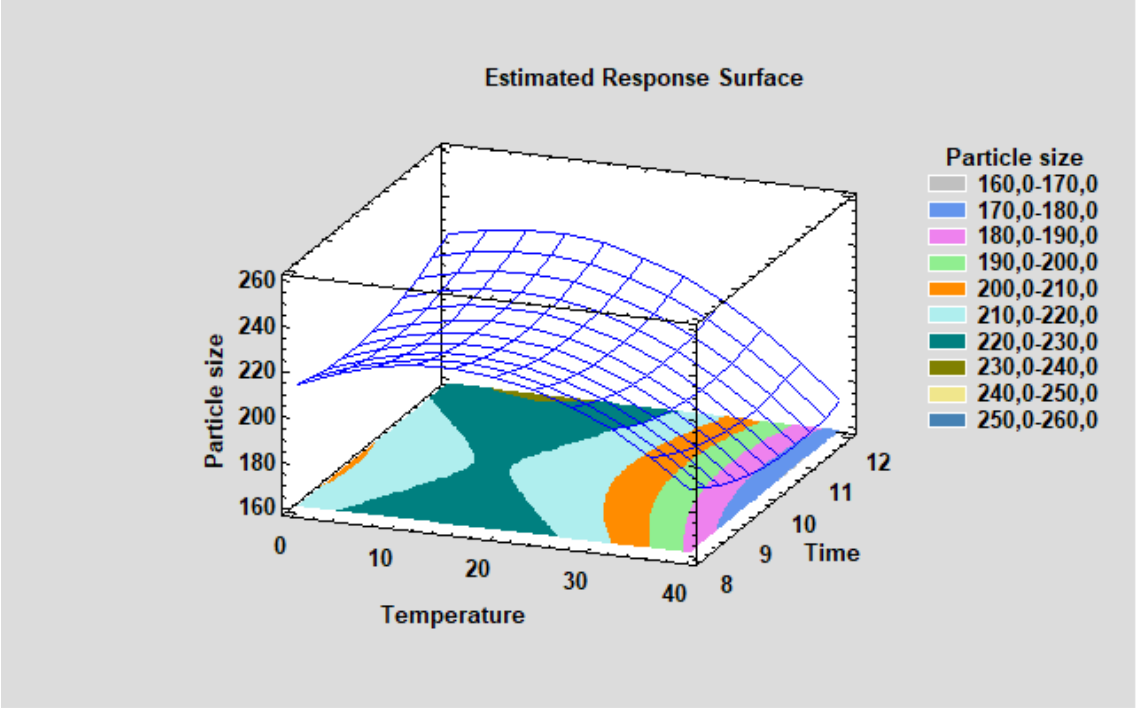

Figure 2

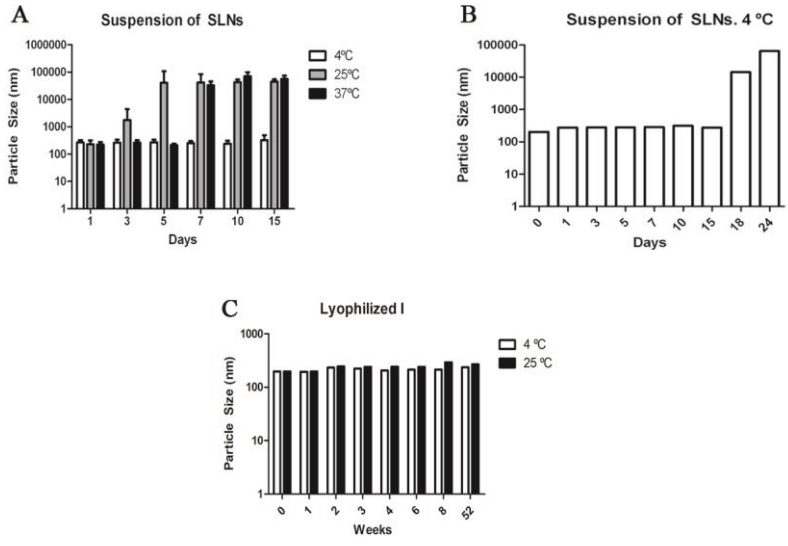

Figure 3

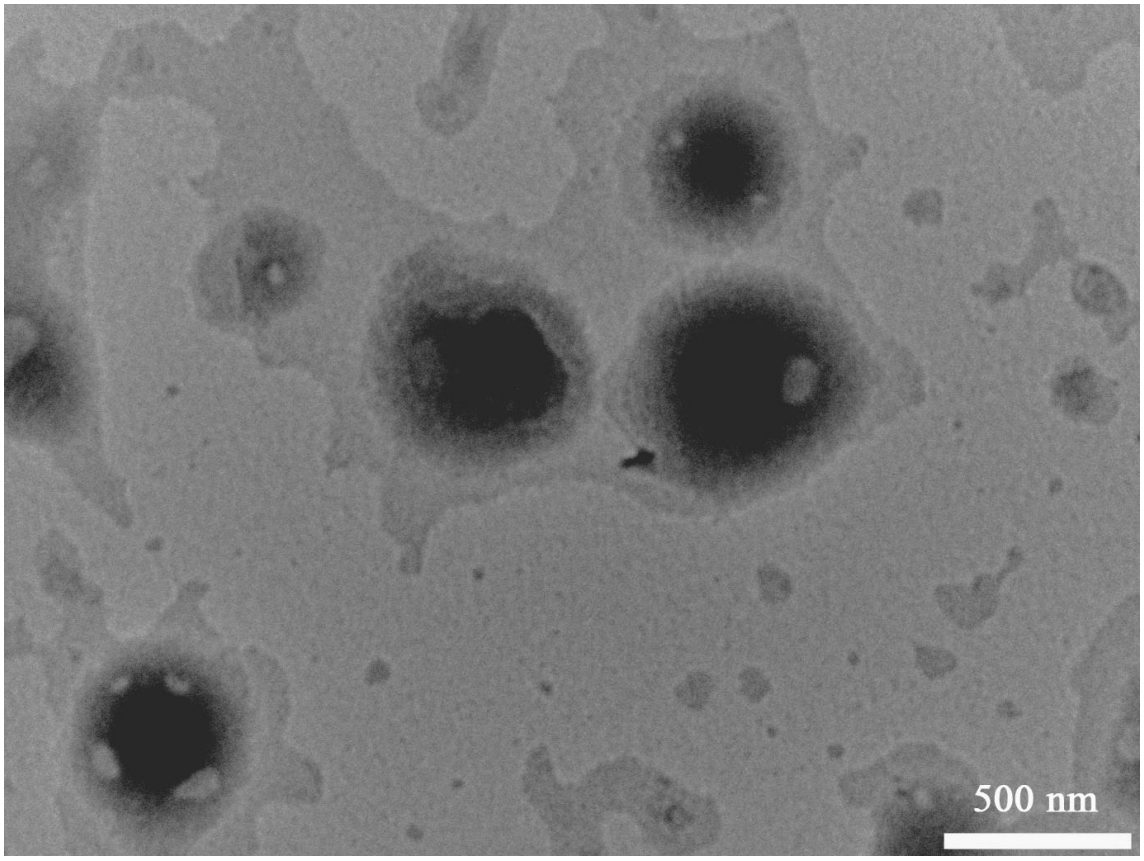

Figure 4

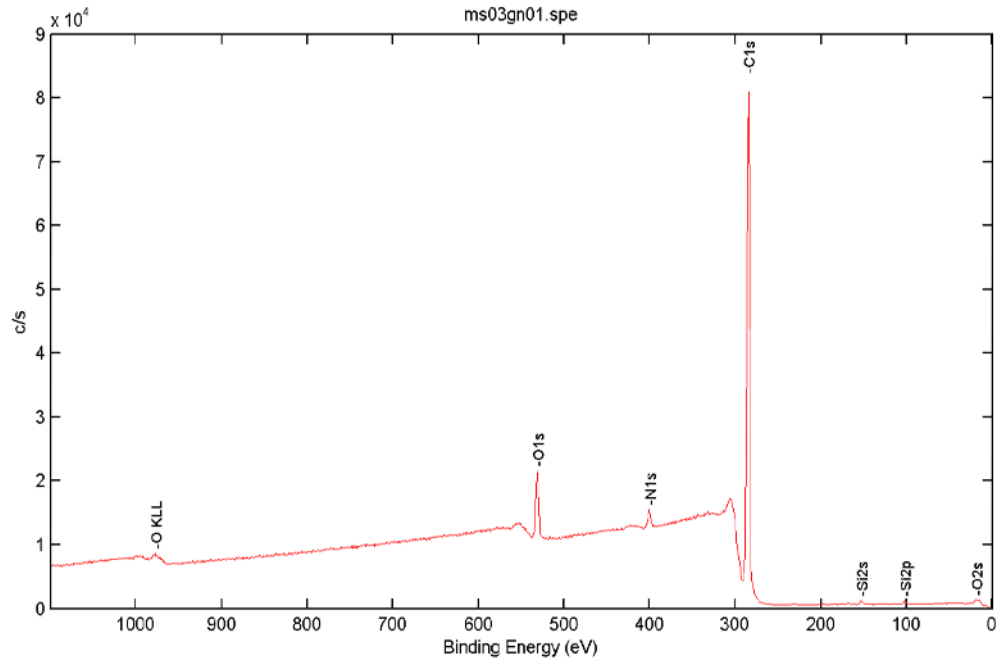

Figure 5

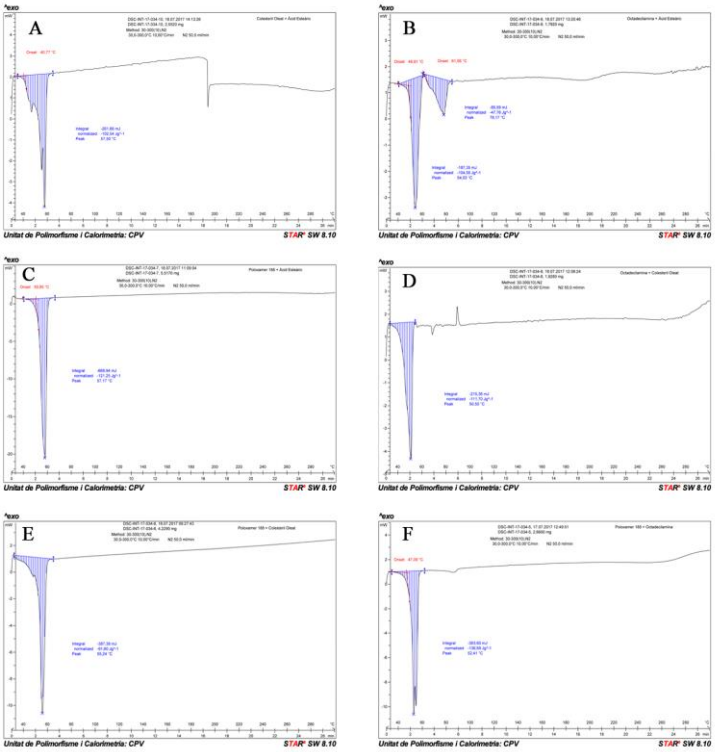

Figure 6

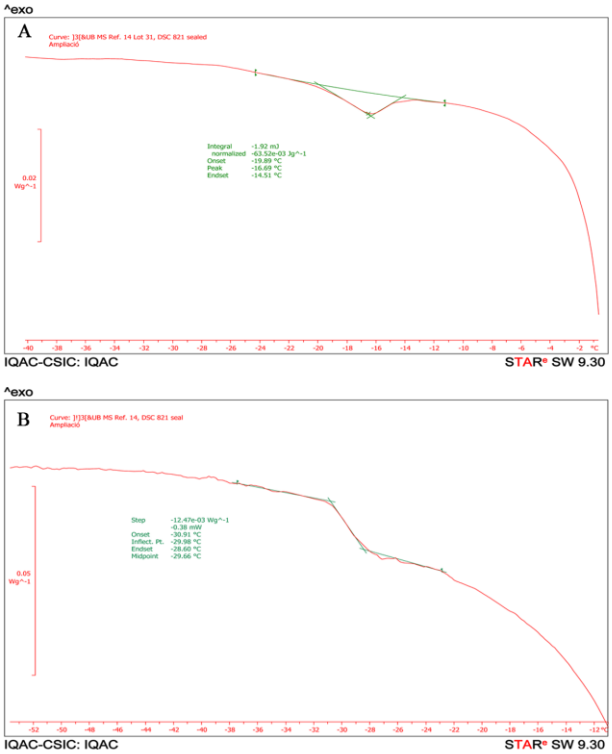

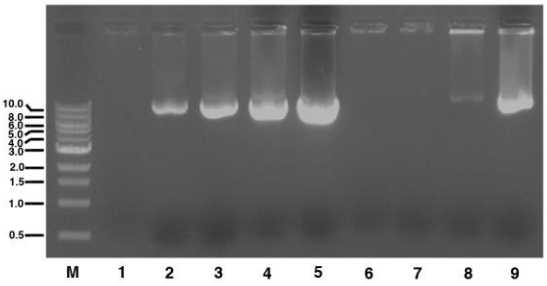

Figure 7

Figure 8